

A multivariate approach for patient specific EEG seizure detection using empirical wavelet transform

Abhijit Bhattacharyya and Ram Bilas Pachori, *Senior member, IEEE*

Abstract—Objective: This paper investigates the multivariate oscillatory nature of electroencephalogram (EEG) signals in adaptive frequency scales for epileptic seizure detection. **Methods:** The empirical wavelet transform (EWT) has been explored for the multivariate signals in order to determine the joint instantaneous amplitudes and frequencies in signal adaptive frequency scales. The proposed multivariate extension of EWT has been studied on multivariate multi-component synthetic signal, as well as on multivariate EEG signals of CHB-MIT scalp EEG database. In a moving window based analysis, two seconds long multivariate EEG signal epochs containing five automatically selected channels have been decomposed and three features have been extracted from each one second part of the two second long joint instantaneous amplitudes of multivariate EEG signals. The extracted features from each oscillatory level have been processed using a proposed feature processing step and joint features have been computed in order to achieve better discrimination of seizure and seizure-free EEG signal epochs. **Results:** The proposed detection method has been evaluated over 177 hours of EEG records using six well known classifiers. We have achieved average sensitivity, specificity and accuracy values as 97.91% and 99.57% and 99.41% respectively, using ten-fold cross-validation method, which are significantly higher than the existing state of art methods studied on this database. **Conclusion:** Efficient detection of epileptic seizure is possible when seizure events appear for long duration in hours long EEG recordings. **Significance:** The proposed method develops time-frequency plane for multivariate signals and builds patient specific models for EEG seizure detection.

Index Terms—Multivariate EEG signal, channel selection, empirical wavelet transform, feature processing, classifiers.

I. INTRODUCTION

EPILEPSY is the second most known (after stroke) neuronal disorder of the brain, caused by simultaneous abnormal firing of a cluster of neurons and affects almost 60 million people worldwide [1]. The detection and diagnosis of epileptic seizures often require long duration monitoring of the patient's electroencephalogram (EEG) signals. However, the manual process of long duration monitoring of the patient's EEG signal is tedious and time consuming task. In addition, the recorded EEG signals may be contaminated with background noise, muscle artifacts, and other neuronal symptomatology. Hence, an automatic seizure detection system would facilitate the real time monitoring and therapy of the epileptic seizures.

Most of the recent studies have set the ultimate objective of developing automated EEG monitoring system to detect epileptic seizures. In [2], Osorio *et al.* presented a seizure

Abhijit Bhattacharyya and Ram Bilas Pachori are with Discipline of Electrical Engineering, Indian Institute of Technology Indore, Indore- 453552, India (e-mail: phd1401202001@iiti.ac.in, pachori@iiti.ac.in).

detection method using wavelet based band-pass finite-impulse response (FIR) filter. The authors generated a foreground sequence from the EEG signal by computing the median of the squared values of each filtered EEG signal epochs. Then, they computed the ratio of foreground to its history and compared with a defined threshold to detect EEG seizures. They also achieved 100% sensitivity and specificity when studied a database of short intracranial EEG segments.

In [3], the authors identified seizure onset patterns by employing a temporal pattern (TP) filter. They selected relevant segments from pre-ictal and ictal durations to find special temporal patterns. The TP filter was then designed from the weighted sum of the special temporal patterns. They applied TP filter to scalp EEG recordings in order to find abstruse seizure patterns.

Epileptic seizure detection with artificial neural network has been explored in several studies. In [4], the authors trained self-organizing map (SOM) neural network with time-frequency representation of reference seizure epochs. Finally, they compared the feature vector of test seizure epochs with the reference neural network vectors and employed a rule based decision sequence to detect epileptic seizures. Later in [5], the method was evaluated on a large surface EEG database. In this study, the reported sensitivity was 92.8% with a false detection rate of 1.35 per hour. In [6], Hesse and James proposed a novel topographical approach based on independent component analysis (ICA) to detect epileptiform activities in multi-channel EEG signals. The authors found sensor projections and source waveforms from a reference EEG segment by employing ICA and hence epileptic seizure was traced by taking the cross-correlation between signal subspace and target-sensor projection using moving-window based method. The preliminary results obtained in this study were very promising when studied on scalp EEG signals of one epilepsy patient.

Shoeb *et al.*, in [7] designed an EEG seizure detector and studied on CHB-MIT scalp EEG benchmark database. They passed the EEG signal epochs of two seconds duration through a filter bank, composed of eight filters, spanning in the range of 0.5 to 25 Hz. Then, the feature vector was formed by measuring the energy of the output of each filter. The procedure was repeated for all the channels. Their method detected 96% of the test seizures with median false detection rate of 2 false detections in 24 hours long EEG recording. Kiranyaz *et al.* [8] proposed a seizure detection method which uses time, frequency, time-frequency, and non-linear features. The authors developed a collective network of binary classifiers along with a novel morphological filtering

TABLE I: Patients information of CHB-MIT benchmark scalp EEG database

PI-Gender-Age	Seizure events- (T _{min} -T _{max}) in seconds	Total seizure time in seconds	Total seizure- free time in seconds
1-F-11	7 (28-102)	449	23475
2-M-11	3 (10-83)	175	7983
3-F-14	7 (48-70)	409	24791
4-M-22	4 (50-117)	382	37976
5-F-7	5 (97-121)	563	17437
6-F-1.5	9 (13-21)	147	93051
7-F-14.5	3 (87-144)	328	32208
8-M-3.5	5 (135-265)	924	17076
9-F-10	4 (63-80)	280	34218
10-M-3	7 (36-90)	454	50008
11-F-12	3 (23-753)	809	9249
13-F-3	12 (18-71)	547	28253
14-F-9	8 (15-42)	117	25023
15-M-16	20 (31-205)	2012	48420
16-F-7	10 (7-15)	94	21506
17-F-12	3 (89-116)	296	10528
18-F-18	6 (31-69)	323	19951
19-F-19	3 (78-82)	239	10307
20-F-6	8 (30-50)	302	19732
21-F-13	4 (13-82)	203	13587
22-F-9	3 (59-75)	207	10593
23-F-6	7 (21-114)	431	31823
24-NR-NR	16 (17-71)	527	42673

for the detection of EEG seizures. They studied their method to long duration CHB-MIT scalp EEG database and reported an average sensitivity of 89.01% with 25% training rate. Later, Zabihi *et al.* in [9], proposed a novel real time seizure detection system which reconstructs seizure and seizure-free segments of EEG signals in higher dimensional space by employing time-delay embedding method. They achieved an average sensitivity of 88.27% using 25% training rate, with a two layered classifier system followed by morphological filtering operation. In [10], authors mapped the scaled EEG signals and their associated frequency sub-bands into two dimensional space which results into a texture image. They applied gray level co-occurrence matrix (GLCM) to extract multivariate textural features followed by several classifiers for the discrimination of seizure and seizure-free EEG signals. They have reported maximum average sensitivity of 70.19% with support vector machine (SVM) classifier.

In recent years, wavelet transform based methods have been applied extensively for analyzing non-stationary signals like EEG. In [11]–[15] authors analyzed the animals EEG signals using continuous wavelet transform (CWT) based approach. In [11] authors used Morlet wavelet and specially generated adoptive wavelets for the detection of spike wave discharges (SWD) (30-50 Hz frequency band) and sleep spindles (SS) (7-14 Hz frequency band) respectively from the EEG signals of WAG/Rij rats. In [12], the CWT based method was developed for the real-time detection of SWD from electrocorticography (ECOG) signals of eight male WAG/Rij rats. The Morlet based CWT was used in [13], for the time-frequency analysis of anterior SS in non-epileptic Wistar and epileptic WAG/Rij rats. In [14], the authors used optimal wavelet parameters in a CWT based serial adaptive method and enhanced the performance

of detection of SS and SWD in WAG/Rij male rat's EEG signals. In [15], several off-line and on-line methods for the detection of SWD in ECoG signals of rodent models have been discussed and a wavelet based method for seizure prediction has been proposed. Majority of the studies in the area of long-term EEG seizure detection have been focused on univariate analysis of EEG signals which do not consider cross-channel interdependence of multivariate data. Moreover, analyzing EEG signals in fixed frequency bands is contrary to its highly non-stationary nature, because complex physiological signals like EEG signal rhythms drift in different frequency bands. An adaptive signal decomposition technique may be useful for decomposing EEG signals into signal adaptive frequency bands. Recently, multivariate modulated oscillation has been proposed for the purpose of modelling the joint oscillatory structure of multichannel signals by utilizing the idea of joint instantaneous frequency and bandwidth in [16]. In [17], the time-frequency analysis of multivariate data has been presented using synchrosqueezing wavelet transform using the idea of joint instantaneous frequency which is proposed in [16]. But synchrosqueezing wavelet transform has the limitation of applicability for long duration signals [18].

Keeping in mind the aforementioned issues, we have extended the concept of empirical wavelet transform (EWT) [19] for the analysis of multichannel signals. The EWT has been applied for the diagnosis of glaucoma in [20]. The authors in [20] decomposed images using two-dimensional (2D) EWT and extracted correntropy features from 2D-EWT decomposed components to classify normal and glaucoma images. In [21], the area parameter have been computed from 2D reconstructed phase space (RPS) projection of EEG rhythms obtained using EWT. The extracted area parameter was used as a feature for the classification of focal and non-focal EEG signals. In this work, we explore EWT for multivariate signals and develops the time-frequency plane for multivariate signals by computing joint instantaneous amplitude and frequency functions from signal adaptive frequency scales. Finally, we investigate joint oscillatory nature of multivariate EEG signals in signal adaptive frequency scales for patient-specific epileptic seizure detection. In order to reduce the processing time, a novel channel selection method has been proposed, which selects five distinct channels based on statistical measures. Multichannel EEG signal epochs of two seconds duration have been decomposed into adaptive frequency sub-bands (MODEs). Then, the amplitude and frequency information of sub-band signals corresponding to each individual channel, which belong to same oscillatory levels have been combined to obtain joint instantaneous amplitude and frequency functions. Afterwards, three features have been extracted from each one second duration of joint instantaneous amplitude function and a novel feature processing has been performed for the detection of epileptic seizures from EEG signals. Finally, the performance of the proposed method has been evaluated using six well known classifiers. The block diagram of the proposed seizure detection algorithm has been shown in Fig. 1.

The rest of the paper is organised as follows. Section II describes the studied EEG database, Section III discusses about the automatic channel selection procedure, Section IV

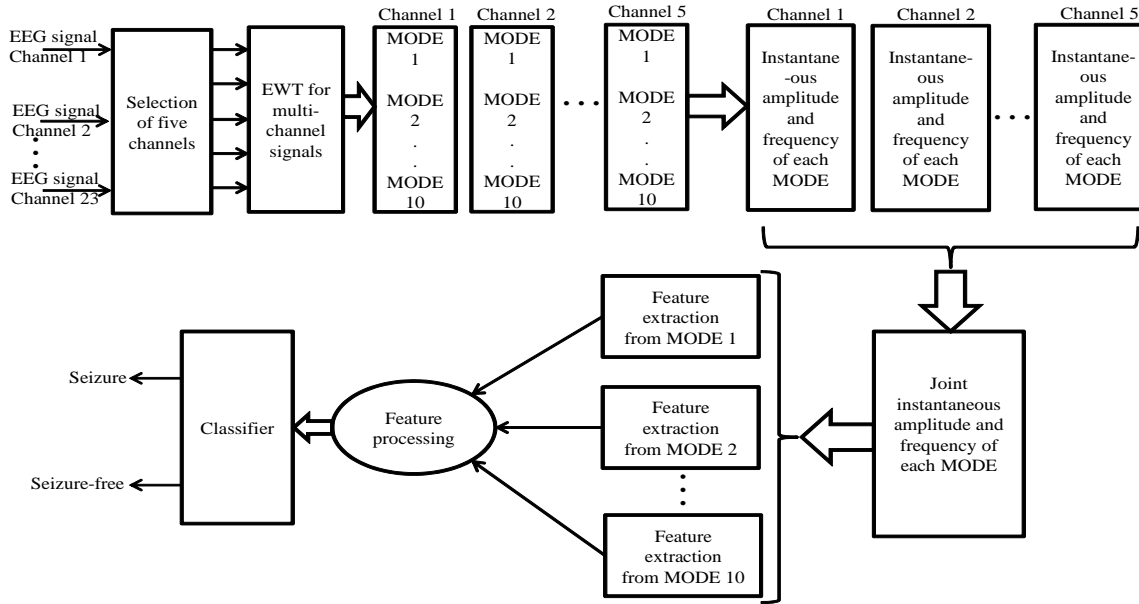


Fig. 1: Proposed multivariate EWT based method for patient-specific EEG seizure detection.

presents the multivariate extension of EWT, Section V gives brief description about the extracted features and an additional feature processing step, Section VI discusses about the classification of EEG records, Section VII presents the experimental results and discusses about the outcome of experiment. Finally, Section VIII concludes the paper.

II. EEG DATASET

Long duration EEG signal records studied in this work have been collected from PhysioNet [22] CHB-MIT scalp EEG database (Website: <https://physionet.org/physiobank/database/chbmit/>), which is described in [23]. The EEG records have been obtained from 23 pediatric patients. Male patients are in the age group of 3 and 22 years, while female patients are in the age group of 1.5 and 19 years. The information about the considered records of the database has been presented in Table I. In Table I, the PI stands for respective patient index, whereas T_{\min} and T_{\max} denote the minimum and maximum seizure duration of the respective patient. The M and F denote male and female subjects respectively. The EEG recordings of patient 1 and patient 21 were acquired from same patient only, with a gap of 1.5 year. The annotations namely seizure and seizure-free were made for all the records with one second resolution. The EEG signals were recorded with a sampling rate of 256 Hz and 16-bit resolution. All the EEG signals were recorded with 23 common EEG channels (FP1-F7, F7-T7, T7-P7, P7-O1, FP1-F3, F3-C3, C3-P3, P3-O1, FP2-F4, F4-C4, C4-P4, P4-O2, FP2-F8, F8-T8, T8-P8, P8-O2, FZ-CZ, CZ-PZ, P7-T7, T7-FT9, FT9-FT10, FT10-T8 and T8-P8),

following the protocol of international 10-20 system of electrode positions. In present study, the records where at least one seizure event is present, has been considered. We failed to read the EEG signals for the patient 12, thus in this study patient 12 has not been considered. In the next section, the channel selection procedure has been explained.

III. CHANNEL SELECTION

Multivariate analysis considers all the EEG channels at the same time. Inclusion of large number of channels in the EEG signal analysis will make the system computationally expensive. In [24], the authors presented a seizure prediction method studied on CHB-MIT scalp EEG database. They found that adaptively selected four to six channels were good enough for the EEG seizure prediction task. For our study, we have selected five distinct channels out of twenty three for multivariate analysis of EEG signals. We have also reported the average performance measures of the proposed method by considering four and six number of channels. The selection procedure can be summarised as follows: Firstly, the channel with least standard deviation (SD) has been considered. The reason behind this could be explained as, the seizure events appear in a long duration EEG recording for very short time interval. Seizure segments are generally distinguished in long term EEG recording, as the spike-rate increases [25] in those intervals and signal amplitude also becomes very high (in all the channels). But because of unwanted artifacts or muscular movement, in some cases, seizure-free intervals in few channels also experience the same. If spike-rate and amplitude increases in seizure-free intervals other

than seizure intervals, then recorded signal in those channels will have comparatively high SD. It is shown in Fig. 2 that channel FT10-T8, where seizure interval (1732 seconds to 1772 seconds) is very prominent, has the least SD among all the 23 channels and the channel FZ-CZ, in which seizure event is hard to identify, has the highest SD in the group of 23 channels. For the purpose of EEG seizure detection using the proposed multivariate extension of EWT, we have been focused to choose the remaining four channels which are highly interdependent or similar to the first selected channel. The mutual information (MI) is used as quantitative measure in order to find the similarity or interdependency of two random variables and is applied for finding the interdependent channels (with the target channel) in multichannel signal prediction algorithm [26]. Thus, the rest of the 4 channels are selected which have higher mutual information (MI) with the channel FT10-T8. Mathematically, the MI of two discrete variables U and V is defined as [27]:

$$MI(U; V) = H(U) + H(V) - H(U, V) \quad (1)$$

where $H(U)$ and $H(V)$ are the computed entropy values of the discrete variables U and V respectively, whereas $H(U, V)$ is the joint entropy of U and V . **It should be noted that entire available lengths of the records have been considered for channel selection purpose.**

In the next section, the concept of EWT for multivariate signals has been explained and applied to multivariate multi-component synthetic signal and real time EEG signals.

IV. MULTIVARIATE EXTENSION OF EMPIRICAL WAVELET TRANSFORM

In this section, firstly the brief theory of EWT has been presented, finally we describe the building blocks for multivariate extension of EWT and its application for analysis of synthetic signal and real EEG signals.

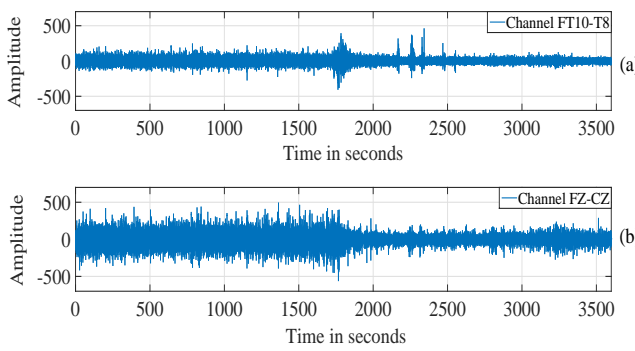


Fig. 2: EEG signals corresponding to two different channels of patient 1.

A. Empirical wavelet transform

The EWT has been proposed in [19] for non-stationary signal analysis. The EWT builds signal adaptive wavelet based

filters. The wavelet based filters are adaptive in the sense that, they have supports in information location in the spectrum of the analyzed signals. The sub-band signals (denoted as MODE) which are obtained from EWT have compact frequency support and centered around a specific frequency, hence satisfies intrinsic mode function (IMF) criteria [19]. Concept of EWT can be summarised as follows [19]:

Step 1: Obtaining the Fourier spectrum in the frequency range $[0, \pi]$ of the analyzed signal by applying fast Fourier transform algorithm. *Step 2:* Segmentation of the Fourier spectrum into N contiguous segments using EWT boundary detection method [19] in order to determine the boundary frequencies $\{\Omega_i\}_{i=0\dots N}$. It should be noted that first (Ω_0) and last (Ω_N) boundary frequencies are 0 and π respectively [19]. The Fourier segments are represented as $[0 \ \Omega_1], [\Omega_1 \ \Omega_2], \dots [\Omega_{N-1} \ \pi]$. *Step 3:* Defining empirical wavelets as the bandpass filters on each segment. For generation of empirical wavelet based filter for each segment, the idea of construction of Littlewood-Paley and Meyer's wavelets [28] has been utilized.

Empirical scaling function and empirical wavelet function can be expressed by (2) and (3), respectively [19].

$$\Gamma_i(\Omega) = \begin{cases} 1, & \text{if } |\Omega| \leq (1 - \theta)\Omega_i. \\ \cos\left(\frac{\pi\Theta(\theta, \Omega_i)}{2}\right), & \text{if } (1 - \theta)\Omega_i \leq |\Omega| \leq (1 + \theta)\Omega_i. \\ 0, & \text{otherwise} \end{cases} \quad (2)$$

$$\Upsilon_i(\Omega) = \begin{cases} 1, & \text{if } (1 + \theta)\Omega_i \leq |\Omega| \leq (1 - \theta)\Omega_{i+1}. \\ \cos\left(\frac{\pi\Theta(\theta, \Omega_{i+1})}{2}\right), & \text{if } (1 - \theta)\Omega_{i+1} \leq |\Omega| \leq (1 + \theta)\Omega_{i+1}. \\ \sin\left(\frac{\pi\Theta(\theta, \Omega_i)}{2}\right), & \text{if } (1 - \theta)\Omega_i \leq |\Omega| \leq (1 + \theta)\Omega_i. \\ 0, & \text{otherwise.} \end{cases} \quad (3)$$

Where,

$$\Theta(\theta, \Omega_i) = \alpha \left(\frac{(|\Omega| - (1 - \theta)\Omega_i)}{2\theta\Omega_i} \right) \quad (4)$$

In above mentioned expressions, the parameter θ makes sure, that empirical scaling function and empirical wavelets form a tight frame in $L^2(\mathbb{R})$. The condition of tight frame can be expressed as follows [19]:

$$\theta < \min_i \left(\frac{\Omega_{i+1} - \Omega_i}{\Omega_{i+1} + \Omega_i} \right) \quad (5)$$

and $\alpha(x)$ is an arbitrary function defined as [19]:

$$\alpha(x) = \begin{cases} 0, & \text{if } x \leq 0. \\ \text{and } \alpha(x) + \alpha(1 - x) = 1, & \forall x \in [0 \ 1] \\ 1, & \text{if } x \geq 1. \end{cases} \quad (6)$$

The approximation and detail coefficients found from the inner product of the applied signal $y(t)$ with the scaling

and wavelet functions. The EWT based time-frequency representation can be obtained after extracting instantaneous amplitudes and frequencies from the filtered sub-band signals by applying the Hilbert transform. There exist several popular methods for obtaining time-frequency representation of non-stationary signals like wavelet skeleton method [29], Hilbert-Huang transform (HHT) method [30], [31] etc. The skeleton representation of the time-frequency plane is more desirable due to availability of quantitative results. Wavelet skeleton is an approach for visualizing the wavelet transform results using local maxima or minima of the wavelet surface at every time instant [29]. In [32], the authors determined wavelet skeleton using local maxima of the continuous wavelet coefficients. This method in ideal case reduces the blurredness of the energy distribution in the time-frequency domain because of redundancy and sub-harmonics. But for complex data, the wavelet skeleton approach is encumbered by the harmonics due to fixed priori basis functions [33]. In HHT based time frequency method, first the IMFs are extracted from the analyzed signal using empirical mode decomposition (EMD) method and then Hilbert transform is applied on each extracted IMF to obtain instantaneous amplitude and frequency [30]. Finally, the instantaneous frequency functions are plotted in the time-frequency plane with an intensity of instantaneous amplitude. In [19], a comparison is made between EWT and HHT based time-frequency representation for synthetic and real seismic signal. It has been observed that low frequency region of HHT time-frequency plane is contaminated with artifacts, while EWT based time frequency representation does not have such problem. This is due to the fact that the decomposition with EMD forces the extraction of IMFs from the components in low frequency region which do not satisfy IMF criteria [19].

B. EWT based multivariate time frequency representation

To extend the concept of EWT for multichannel signals, MODEs, which can be considered as amplitude and frequency modulated (AFM) components for each channel need to be extracted. Then, we can find the joint instantaneous frequency at each oscillatory level following the condition that the frequencies of the MODEs falling in the same level for each individual channel are sufficiently close together. The prime task is to find matched mono-component signals from multichannel signals.

Let the multivariate time series be represented as in (7):

$$y(t) = \begin{bmatrix} y_1(t) \\ y_2(t) \\ \vdots \\ y_M(t) \end{bmatrix} \quad (7)$$

As EWT generates adaptive wavelet based bandpass filters, the MODEs of EEG signals corresponding to different channels will differ in number and their frequency range also will be different, this puts an obstacle for multivariate analysis. To overcome the issue, we have computed the mean spectrum magnitude of EEG signals obtained from all the channels which is defined as:

$$Y(f) = \frac{1}{M} \sum_{m=1}^M |Y_m(f)| \quad (8)$$

Where $Y_m(f)$ is the Fourier spectrum of each individual channel and M is the number of channels. The parameter m varies from 1 to M . Then, the boundary search method described in the previous subsection has been applied to the mean spectrum magnitude $Y(f)$ to generate the adaptive wavelet based filter bank. The next step is to decompose all the channels with the generated filter bank. In this case, number of MODEs will be same for each channel and the MODEs generated for each channel will have same frequency support in every oscillatory level.

After decomposing the multivariate signal $y(t)$, the multivariate signal representation can be given as follows:

$$y(t) = \begin{bmatrix} y_1, \text{ MODE}_1(t) & y_1, \text{ MODE}_2(t) & \cdots & y_1, \text{ MODE}_N(t) \\ y_2, \text{ MODE}_1(t) & y_2, \text{ MODE}_2(t) & \cdots & y_2, \text{ MODE}_N(t) \\ \vdots & \vdots & \ddots & \vdots \\ y_M, \text{ MODE}_1(t) & y_M, \text{ MODE}_2(t) & \cdots & y_M, \text{ MODE}_N(t) \end{bmatrix} \quad (9)$$

where, N is the number of decomposition levels for each individual channel. The variable n varies from 1 to N . These MODEs are narrow-band components, so the Hilbert transform is a suitable tool for determining instantaneous amplitude and frequency of each MODE. The analytic signal representation of each MODE, $y_{m,n}(t)$ is defined using Hilbert transform operator (\mathcal{H}) as [30]:

$$y_{+(m, \text{ MODE}_n)}(t) = y_{m, \text{ MODE}_n}(t) + j\mathcal{H}(y_{m, \text{ MODE}_n}(t)) \quad (10)$$

Equation (10) can also be expressed as,

$$y_{+(m, \text{ MODE}_n)}(t) = A_{(m, \text{ MODE}_n)}(t)e^{j\phi_{m, \text{ MODE}_n}(t)} \quad (11)$$

The instantaneous amplitude $A_{(m, \text{ MODE}_n)}(t)$ is defined as,

$$A_{(m, \text{ MODE}_n)}(t) = \sqrt{(y_{m, \text{ MODE}_n}(t))^2 + (\mathcal{H}(y_{m, \text{ MODE}_n}(t)))^2} \quad (12)$$

The instantaneous phase $\phi_{m, \text{ MODE}_n}(t)$ is defined as,

$$\phi_{m, \text{ MODE}_n}(t) = \arctan \left[\frac{\mathcal{H}(y_{m, \text{ MODE}_n}(t))}{y_{m, \text{ MODE}_n}(t)} \right] \quad (13)$$

The instantaneous frequency $f_{m, \text{ MODE}_n}(t)$, is defined as,

$$f_{m, \text{ MODE}_n}(t) = \frac{d}{dt} [\phi_{m, \text{ MODE}_n}(t)] \quad (14)$$

Now the multivariate signal $y(t)$ can be expressed by multivariate instantaneous amplitude $A(t)$ and multivariate instantaneous frequency $f(t)$ as follows:

$$A(t) = \begin{bmatrix} A_1, \text{ MODE}_1(t) & A_1, \text{ MODE}_2(t) & \cdots & A_1, \text{ MODE}_N(t) \\ A_2, \text{ MODE}_1(t) & A_2, \text{ MODE}_2(t) & \cdots & A_2, \text{ MODE}_N(t) \\ \vdots & \vdots & \ddots & \vdots \\ A_M, \text{ MODE}_1(t) & A_M, \text{ MODE}_2(t) & \cdots & A_M, \text{ MODE}_N(t) \end{bmatrix} \quad (15)$$

$$f(t) = \begin{bmatrix} f_1, \text{ MODE}_1(t) & f_1, \text{ MODE}_2(t) & \cdots & f_1, \text{ MODE}_N(t) \\ f_2, \text{ MODE}_1(t) & f_2, \text{ MODE}_2(t) & \cdots & f_2, \text{ MODE}_N(t) \\ \vdots & \vdots & \ddots & \vdots \\ f_M, \text{ MODE}_1(t) & f_M, \text{ MODE}_2(t) & \cdots & f_M, \text{ MODE}_N(t) \end{bmatrix} \quad (16)$$

Now the columns of (15) and (16), which are instantaneous amplitudes and frequencies respectively, belong from distinct oscillatory level $\{f_n\}_{n=1 \dots N}$. It should be noted that at each point of time, instantaneous frequencies of different oscillatory levels are well separated, expressed as $f_m, \text{ MODE}_n(t) > f_{m-1}, \text{ MODE}_n(t)$. In the next step, instantaneous amplitudes and frequencies across all the channels (M) could be combined. The joint instantaneous frequency denoted by $f_n^{\text{multi}}(t)$ and joint instantaneous amplitude denoted by $A_n^{\text{multi}}(t)$ of all the channels in distinct oscillatory levels are defined as follows [16], [17]:

$$f_n^{\text{multi}}(t) = \frac{\sum_{m=1}^M [A_m, \text{ MODE}_n(t)]^2 f_m, \text{ MODE}_n(t)}{\sum_{m=1}^M [A_m, \text{ MODE}_n(t)]^2} \quad (17)$$

$$A_n^{\text{multi}}(t) = \sqrt{\sum_{m=1}^M [A_m, \text{ MODE}_n(t)]^2} \quad (18)$$

The multivariate time-frequency coefficients in each oscillatory level can be computed as follows [17]:

$$\text{TF}_n^{\text{multi}}(f, t) = A_n^{\text{multi}}(t) \delta[f - f_n^{\text{multi}}(t)] \quad (19)$$

Finally, the multivariate time-frequency coefficients, considering all the oscillatory levels can be expressed as [17]

$$\text{TF}^{\text{multi}}(f, t) = \text{TF}_n^{\text{multi}}(f, t) \text{ for } n = 1 \dots N \quad (20)$$

1) Time-frequency representation of multivariate synthetic signal: Here we have shown the performance of the proposed multivariate extension of EWT, when applied to bivariate multi-component AFM signal [17] as an example of multivariate multi-component non-stationary signal denoted as $x(t)$.

$$x(t) = \begin{bmatrix} x_1(t) + x_2(t) \\ x_3(t) + x_4(t) \end{bmatrix}$$

where

$$\begin{aligned} x_1(t) &= \sin[2\pi(30t + 4\sin(t))] \\ x_2(t) &= \sin[2\pi((30 + \Delta)t + 4\sin(t))] \\ x_3(t) &= [1 + 0.3\sin(2\pi t)]\cos(2\pi 10t) \\ x_4(t) &= [1 + 0.3\sin(2\pi t)]\cos[2\pi(10 + \Delta)t] \end{aligned}$$

The signal present in the first channel is a multi-component frequency modulated (FM) signal, shown in Fig. 3(a), with components $x_1(t)$ and $x_2(t)$. The signal $x_2(t)$ has a frequency deviation of $\Delta = 0.3 \text{ Hz}$. The second channel is a multi-component amplitude modulated (AM) signal, shown in Fig. 3(b) with components $x_3(t)$ and $x_4(t)$. The carrier of $x_4(t)$

also has a frequency deviation of 0.3 Hz . The multivariate time-frequency representation is shown in Fig. 3(c). From the figure it is clear that sinusoidally modulated FM signal in channel 1 posses time-varying frequency components. On the other hand, the solid straight line across 10 Hz in the time-frequency plane clearly presents the constant frequency of amplitude modulated (AM) signal associated with channel 2. Thus, the proposed extension of EWT is able to present the joint oscillatory structure of multivariate multi-component synthetic signals.

2) Time-frequency representation of multivariate EEG signal: The proposed method has been applied to the multivariate EEG signal obtained from five selected channels of CHB-MIT benchmark scalp EEG database. Fig. 4 shows joint instantaneous amplitudes and frequencies of the multivariate EEG signal of two seconds duration in different oscillatory levels. Fig. 5(a) and 5(b) show the time-frequency representation of multivariate EEG signal of seizure and seizure-free segments of four seconds duration respectively. It is observed that multivariate seizure EEG signals have significant energy in high frequency region in the time-frequency plane as compared to multivariate seizure-free EEG signals. In previous studies [34]–[36], authors have suggested that two second long EEG epoch is sufficient to obtain the estimate of the lowest frequency and can be considered stationary signal. Thus, in this work two second long multivariate EEG epochs are decomposed using multivariate extension of EWT and features are extracted from each one second half of the two second long joint instantaneous amplitude function. In the proposed method of selection of channels, out of five selected channels, last four channels are chosen which have relatively higher MI with the first selected channel (have least SD among all available channels). As a result, the selected channels are assumed to be correlated, as MI measures the generalized correlation of time series [27], [37]. Thus spectral compositions of the two second long EEG epochs of the considered channels do not change significantly.

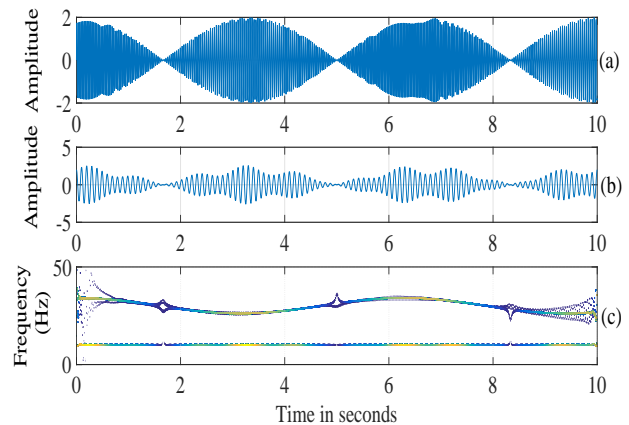


Fig. 3: (a) Sinusoidally modulated multi-component FM signal of channel 1. (b) multi-component AM signal of channel 2 with 0.3 as modulation index. (c) Time-frequency representation of multivariate multi-component synthetic signal.

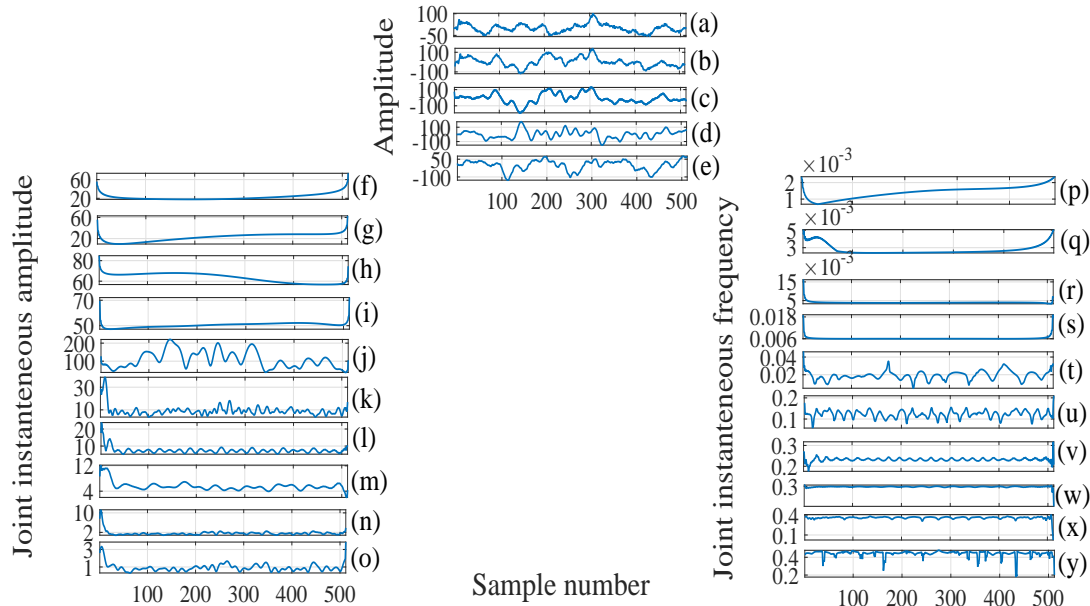


Fig. 4: ((a)-(e)) Multivariate EEG signal of five selected channels and its joint instantaneous amplitudes ((f)-(o)) and frequencies ((p)-(y)). Top to bottom according to ascending order of frequency.

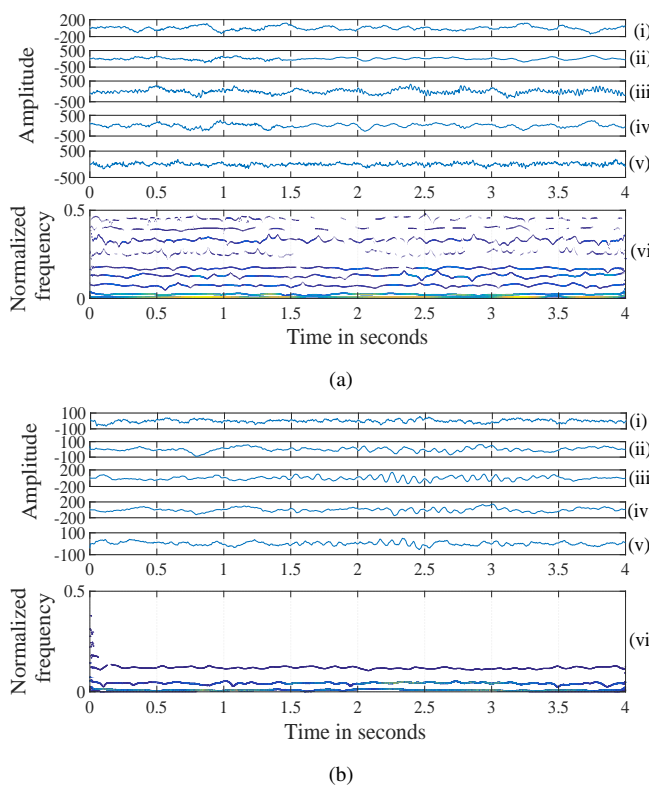


Fig. 5: (a) Plots of the multivariate seizure EEG signal (i-v) of five selected channels and their joint time-frequency representation (vi). (b) Plots of the multivariate seizure-free EEG signal (i-v) of five selected channels and their joint time-frequency representation (vi).

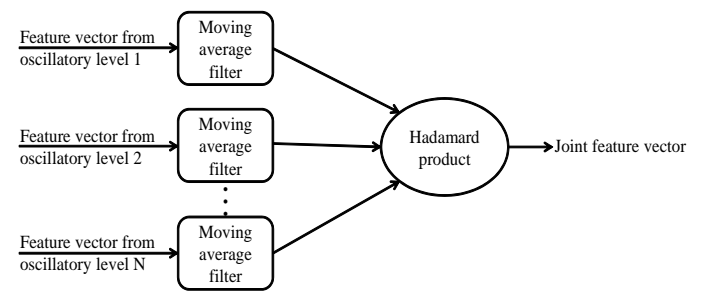


Fig. 6: Proposed framework for feature processing.

V. FEATURE EXTRACTION AND FEATURE PROCESSING

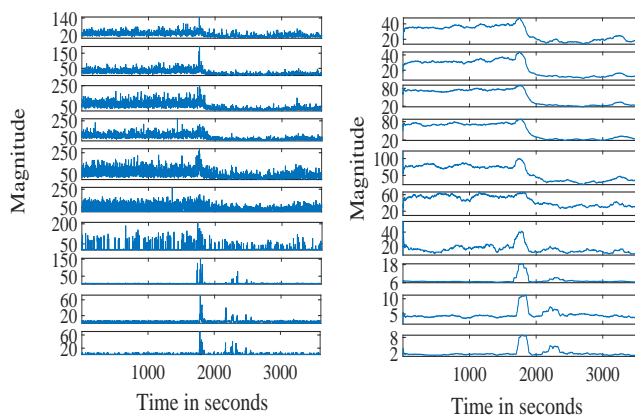
We have extracted three features from the joint instantaneous amplitudes of one second duration, belonging to different oscillatory levels of multivariate EEG signal. The extracted features are as follows:

- 1) Mean of joint instantaneous amplitude which is expressed as follows:

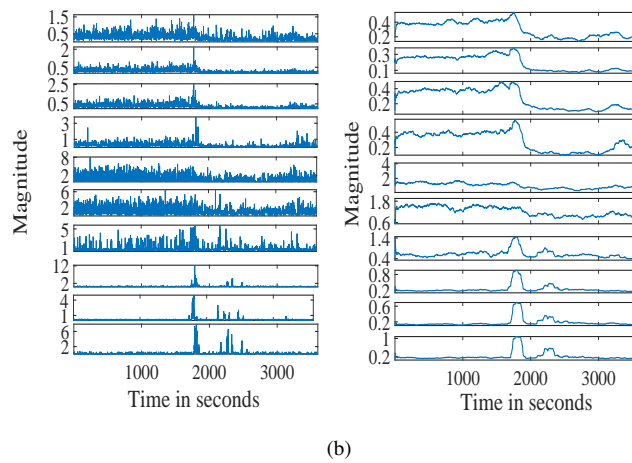
$$\mu = \frac{1}{T} \int_T A_n^{\text{multi}}(t) dt \quad (21)$$

- 2) Mean monotonic absolute AM change can be given as follows [38]:

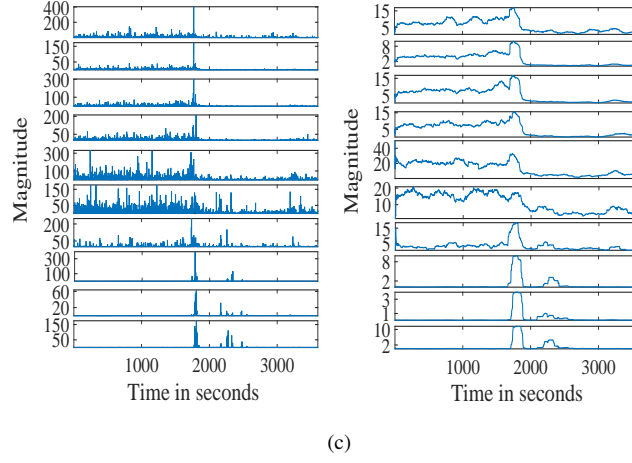
$$\nu = \frac{1}{T} \int_T \left| \frac{dA_n^{\text{multi}}(t)}{dt} \right| dt \quad (22)$$



(a)



(b)



(c)

Fig. 7: (a) Plots of FVs of successive joint oscillatory levels, corresponding to the mean of joint instantaneous amplitude, before (left column) and after (right column) applying moving average filter respectively. (b) Plots of FVs of successive joint oscillatory levels, corresponding to mean monotonic absolute AM change, before (left column) and after (right column) applying moving average filter respectively. (c) Plots of FVs of successive joint oscillatory levels, corresponding to variance of monotonic AM change, before (left column) and after (right column) applying moving average filter respectively.

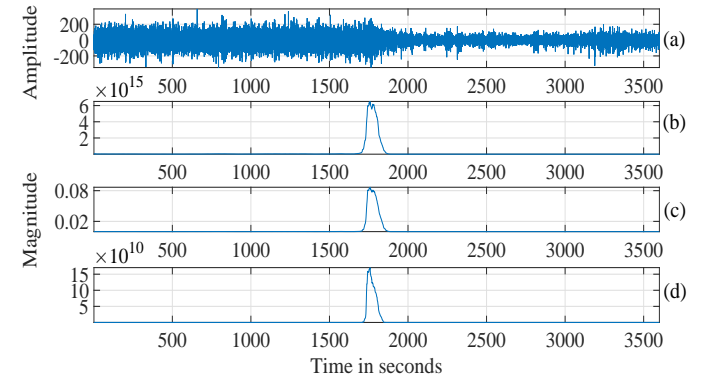


Fig. 8: Plots of (a) raw EEG signal and (b), (c), (d) JFV1, JFV2 and JFV3 respectively.

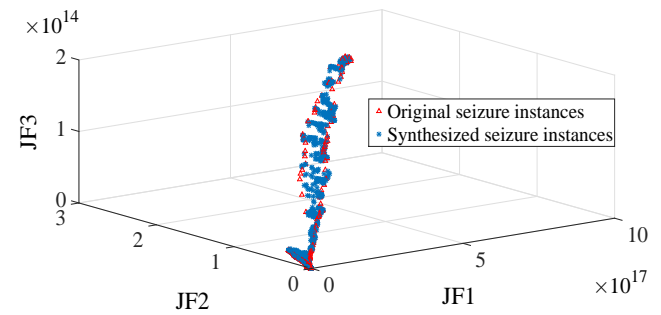


Fig. 9: Original and synthesized seizure instances for patient 1.

3) Variance of monotonic AM change which can be expressed as follows [38]:

$$\sigma = \frac{1}{T} \int_T \left(\frac{dA_n^{\text{multi}}(t)}{dt} - \nu \right)^2 dt \quad (23)$$

Where $A_n^{\text{multi}}(t)$ is the joint instantaneous amplitude in oscillatory level f_n and T is the duration of EEG epochs. In the next step, in order to increase the discrimination between seizure and seizure-free events of EEG signal and to reduce the noise level in seizure-free segment, a novel feature processing stage has been introduced and its block diagram representation is shown in Fig. 6. A moving average filter of window length 150 seconds has been applied on each individual feature vector denoted by FV1, FV2 and FV3 respectively which are formed by concatenating the features computed from successive EEG signal epochs. Figs. 7(a), 7(b), 7(c) show the concatenated features before and after moving average filtering, where the seizure segment (1732-1772 seconds) in most of the oscillatory levels is enhanced. The use of moving average filtering enhances the magnitude of the features which are extracted from seizure segments in most of the oscillatory levels. It should be noted that this type of filtering also enhances the magnitude of features corresponding to seizure-free segments in certain time intervals but only in few oscillatory levels. This may lead to false detection of epileptic seizures. To resolve the

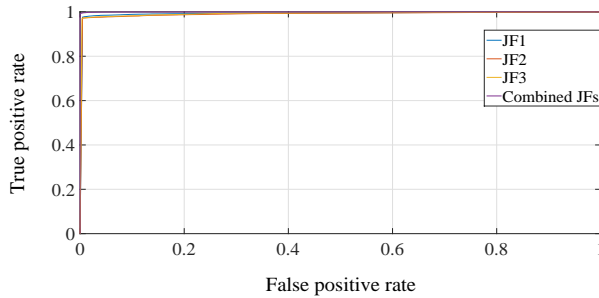


Fig. 10: ROC curves of patient1 for different features.

issue, the joint feature vectors (JFV) have been obtained by computing the Hadamard product of the individual FVs of different oscillatory levels as follows:

$$JFV1 = [\mu_1^{\text{comb}} \mu_2^{\text{comb}} \cdots \mu_P^{\text{comb}}]$$

$$JFV2 = [\nu_1^{\text{comb}} \nu_2^{\text{comb}} \cdots \nu_P^{\text{comb}}]$$

$$JFV3 = [\sigma_1^{\text{comb}} \sigma_2^{\text{comb}} \cdots \sigma_P^{\text{comb}}]$$

Each element of JFV1, JFV2 and JFV3 are the joint features (JF) represented as:

$$\mu_{ep}^{\text{comb}} = \prod_{j=1}^N \mu_{ep}^j, \quad \nu_{ep}^{\text{comb}} = \prod_{j=1}^N \nu_{ep}^j$$

$$\text{and } \sigma_{ep}^{\text{comb}} = \prod_{j=1}^N \sigma_{ep}^j \quad \text{where } ep = 1, 2, \dots, P$$

where ep , N and P represent the epoch number, number of oscillatory levels and total number of epochs respectively.

This operation has two major benefits, firstly after Hadamard product feature magnitude in seizure segments get enhanced and at the same time the magnitude of features in the seizure-free interval becomes substantially less as compared to the magnitude of the features in the seizure interval which result into a better resolution of seizure event in the record, as shown in Fig. 8. Secondly, the dimension of the final feature vector gets reduced, which in turn reduces the risk of over-fitting of the classifiers. Finally, these JFs are fed to the classifiers for performance evaluation of the proposed method as discussed in the next section.

VI. CLASSIFICATION OF EEG RECORDS

The previous section discusses about the multivariate feature extraction and the proposed feature processing technique for better discrimination of seizure and seizure-free EEG segments. It should be noted that, even after considering the records of CHB-MIT scalp EEG database where at least one seizure event is present, the total duration of seizure (10218 seconds) is only 1.6% of total duration of EEG records (640086 seconds). This makes the database highly imbalanced. As a consequence, the classifiers will be biased to detect majority class because of the unequal prior probabilities of the two classes. Generally, two methods namely, over-sampling and under-sampling are used frequently to resolve class imbalance problem [39]. The over-sampling has the advantage of correcting the bias in the database without loosing any information. Therefore, most of the pattern classification methods choose over-sampling as the best option to deal

with skew class distribution [39]. In this study, we have applied a well known method namely, the synthetic minority over-sampling technique (SMOTE) [40] to resolve the class imbalance problem of seizure and seizure-free epochs, which neither exaggerate the receiver operating characteristic (ROC) curve of the extracted features, nor cause any over-fitting problem [41]. In this study, we have applied 3 iterations of SMOTE for each patient, where each iteration increases the number of minority samples by 100%. It is shown in Fig. 9 that synthetically introduced seizure instances are in the cluster of original seizure instances. Finally, the robustness of the proposed feature extraction method has been evaluated using six well known classifiers namely: Random forest (RF) [42], C4.5 [43], functional tree (FT) [44], Bayes-net [45], Naive-Bayes [46], and K-nearest neighbours (K-NN) [47] classifiers which are available at Waikato environment for knowledge analysis (WEKA) software [48].

VII. EXPERIMENTAL RESULTS AND DISCUSSION

We have applied ten-fold cross-validation method [49] to evaluate our proposed feature extraction method. The application of cross-validation method in patient specific seizure detection is not uncommon in the literature [50], [51], as it avoids the problem of over-fitting and gives an unbiased performance of the classifiers. Once a classification model is developed for a specific patient using the proposed method, the same model could be used repeatedly for the upcoming EEG signal records, which in turn will reduce the neurologist's burden of monitoring long duration EEG records. For the performance evaluation of the classifiers, we have computed three well known parameters [52], [53], called sensitivity ($\text{Sens} = \text{TP}/(\text{TP} + \text{FN})$), specificity ($\text{Spec} = \text{TN}/(\text{TN} + \text{FP})$), accuracy ($\text{Acc} = (\text{TP} + \text{TN})/(\text{TP} + \text{TN} + \text{FP} + \text{FN})$).

Where TP (True positive) is the number of truly detected seizure epochs, FN (False negative) is the number of misclassified seizure epochs, TN (True negative) is the number of truly classified seizure-free epochs, FP (False positive) is the number of misclassified seizure-free epochs. Table II presents the patient specific confusion matrix when the proposed method is evaluated with RF, linear Naive Bayes and K-NN classifiers. We have reported the area under the ROC curve (AUC) as a performance measure [52] of the proposed algorithm. As it has been shown in Table III that, with 10-fold cross-validation the proposed method has achieved maximum average sensitivity of 97.91% and maximum average specificity of 99.57% using RF classifier with five adaptively selected EEG channels. The performance of the proposed method slightly falls with four and six number of channels when evaluated with same RF classifier. We have achieved approximately same average sensitivity rate of 97.64% and specificity rate of 99.56% with four and six number of considered channels. Thus, we have considered five EEG channels for the analysis. For most of the patients, the proposed method has performed with high specificity rate and at the same time with moderate sensitivity. The highest sensitivity 99.9% has been achieved for patient 11, at the same time the algorithm achieved a specificity rate of 99.7% using RF classifier. The highest specificity rate of

TABLE II: Patient specific confusion matrix for the proposed seizure detection method using RF, Naive Bayes and k-NN classifiers.

Patient index	RF			Naive-Bayes			K-NN					
	Truly detected seizure (TP)	Misclassified seizure (FN)	Truly detected seizure-free (TN)	Misclassified seizure-free (FP)	Truly detected seizure (TP)	Misclassified seizure (FN)	Naive-Bayes seizure-free (TN)	Misclassified seizure-free (FP)	Truly detected seizure (TP)	Misclassified seizure (FN)	Naive-Bayes seizure-free (TN)	Misclassified seizure-free (FP)
1	3571	21	23378	97	3591	1	22867	608	3502	90	23305	170
2	1396	4	7954	29	1363	37	7820	163	1382	18	7928	55
3	3246	26	24702	89	3109	163	23854	937	3189	83	2450	241
4	3038	18	37916	60	2640	416	36794	1182	2973	83	37826	150
5	4445	59	17332	105	4385	119	16306	1131	4361	143	17250	187
6	1093	83	92989	62	710	466	92532	519	913	263	92680	371
7	2619	5	32154	54	2622	2	31808	400	2601	23	32136	72
8	7361	31	16933	143	6256	1136	16231	845	7223	169	16865	211
9	2234	6	34186	32	2237	3	34061	157	2191	49	34129	89
10	3584	48	49931	77	3298	334	49251	757	3283	349	49411	597
11	6463	9	9222	27	6313	159	8947	302	6448	24	9209	40
13	4151	225	28095	158	3162	1214	27266	987	3845	531	27503	750
14	1364	52	24951	72	881	535	24712	3111	1276	140	24825	198
15	14522	154	47233	187	10936	5160	38823	9597	12522	3574	44173	4247
16	698	54	21450	56	640	112	21170	336	660	92	21355	151
17	2358	10	10500	28	2273	95	10138	390	2321	47	10399	129
18	2553	31	19897	54	2275	309	18479	1472	2398	186	19704	247
19	1907	5	10268	39	1909	3	10161	146	1907	5	10262	45
20	2388	28	19664	68	2395	21	19157	575	237	39	19644	88
21	1598	26	13543	44	1615	9	12540	1047	1567	57	13445	142
22	10537	56	1638	18	1592	64	9272	1321	1609	47	10524	69
23	3430	18	31769	54	3082	366	30548	1275	3414	34	31747	76
24	4092	124	42544	129	2953	1263	41721	952	3682	534	42075	598

TABLE III: Evaluated classification performance parameters with 10-fold cross-validation using six different classifiers.

Patient index	RF			C4.5			FT			Bayes-net			Naive-Bayes			K-NN			
	Spec	Sens	Acc	AUC	Spec	Sens	Acc	AUC	Spec	Sens	Acc	AUC	Spec	Sens	Acc	Spec	Sens	Acc	
1	99.6	99.4	99.6	1	99.3	98.8	99.2	0.995	99.5	97.7	99.2	0.99	98.7	98.1	0.98	97.4	99.9	97.5	0.984
2	99.6	99.7	99.6	1	99.4	99.1	99.4	0.993	99.3	97.9	99.1	0.988	99.1	98.9	0.998	98.9	97.4	0.996	99.2
3	99.6	99.2	99.6	0.999	99.5	98.6	99.4	0.994	99.6	98.3	99.4	0.99	98.7	98.1	0.996	96.2	99.3	98.7	0.991
4	99.8	99.4	99.8	1	99.6	98.8	99.6	0.995	99.6	98.6	99.7	0.994	99.2	88.9	0.984	86.4	96.1	0.989	99.6
5	99.4	98.7	99.3	0.999	99	97.6	98.7	0.993	99.1	97.7	98.8	0.989	97.6	97.4	0.996	93.5	97.4	0.989	98.9
6	99.9	92.9	99.8	0.998	99.9	92.1	99.8	0.984	99.9	88	99.7	0.952	99.9	80.9	0.997	99.4	60.4	0.984	99.6
7	99.8	99.8	99.8	1	99.8	99.5	99.8	0.998	99.8	99.7	99.6	0.998	99.7	99.7	0.988	98.8	99.9	0.999	99.1
8	99.2	99.6	99.3	0.999	98.9	98.9	98.9	0.993	98.9	98.9	99.1	0.991	97.9	96.8	0.996	95.1	84.6	0.98	98.8
9	99.9	99.7	99.9	1	99.9	99.6	99.8	0.998	99.8	98.7	99.7	0.993	99.7	99.7	0.999	99.5	99.9	0.999	97.8
10	99.8	98.7	99.8	0.999	99.7	98.2	99.6	0.992	99.7	97.1	99.5	0.986	99.6	95.8	0.994	98.5	90.8	0.995	98.8
11	99.7	99.9	99.8	1	99.7	99.7	99.8	0.998	99.7	99.7	99.9	0.999	99.7	99.3	0.999	97.5	97.1	0.996	99.6
13	99.4	94.9	98.8	0.998	98.4	88.7	97.1	0.976	98.6	89.9	97.4	0.954	98.2	85.7	0.986	96.5	72.3	0.962	97.3
14	99.7	96.3	96.3	0.998	99.4	90.5	98.9	0.98	99.5	91.9	99.1	0.965	98.8	89.3	0.993	98.8	62.2	0.982	99.2
15	97.5	90.2	95.7	0.991	92.6	73	87.7	0.924	95.6	81.6	92.1	0.899	92.9	71.3	0.934	80.2	67.9	0.843	91.2
16	99.7	92.8	99.5	0.997	99.6	91	99.3	0.977	99.6	85.5	99.1	0.937	99.5	80.3	0.989	98.4	85.1	0.99	99.3
17	99.7	99.6	99.7	1	99.4	99.3	99.4	0.995	99.6	99.1	99.5	0.995	99.2	96.6	0.998	98.9	93.1	0.986	98.7
18	99.7	98.8	99.6	1	99	91.6	98.1	0.99	99.6	96.3	99.2	0.983	99.1	90	0.995	92.6	88	0.921	97.5
19	99.6	99.7	99.6	1	99.5	99.3	99.5	0.996	99.7	98.5	99.5	0.991	99.1	99.7	0.996	98.6	99.8	0.996	99.7
20	99.7	98.3	99.6	1	99.6	98.6	99.5	0.992	99.4	97.6	99.2	0.988	99.5	97.3	0.992	97.1	99.1	0.997	99.6
21	99.7	98.4	99.5	0.999	98.8	92.4	98.1	0.989	99.2	95	98.8	0.975	98.4	90.9	0.995	92.3	99.4	0.986	98.9
22	99.5	98.9	99.4	1	98.9	97.5	98.9	0.989	99.1	97.8	98.9	0.987	97.8	88.9	0.998	96.6	87.5	0.992	98.7
23	99.8	99.5	99.8	1	99.7	98.7	99.6	0.996	99.6	98.1	99.5	0.989	99.4	90.9	0.997	95.3	89.4	0.988	99.8
24	99.7	97.1	99.5	0.998	99.4	93.7	98.9	0.986	99.4	94.6	99	0.975	98.9	85.1	0.997	97.6	70	0.953	98.6
Average	99.57	97.91	99.41	0.999	99.09	95.44	98.64	0.988	98.98	99.30	95.58	0.989	98.70	91.93	0.993	95.74	88.46	0.9516	98.35
																		0.964	

TABLE IV: Comparison of existing seizure detection methods and the proposed method studied on CHB-MIT database.

Reference and year	Method	Considered number of Patients-Channels	Crossvalidation method and training rate	Average Spec%-Sens%-Accu%
Rafiquddin et al. [54] [2011]	Median absolute deviation, interquartile range computed from raw EEG signal along with the energy and coefficients of variation computed from wavelet coefficients (db4)	23-23	No cross-validation, 80% data for training	NR-NR-80.16
Khan et al. [55] [2012]	Relative values of energy and normalized coefficients of variation (NCOV) were computed from wavelet coefficients	5-NR	No cross-validation, 80% data for training	100-83.6-91.8
Hunyadi et al. [56] [2012]	Total 16 features were extracted from time and frequency domain	23-NR	Approximately 80% training	NR-83-NR
Supratak et al. [57] [2014]	Stacked autoencoders were used for unsupervised feature learning	6-NR	30 epochs were used	NR-100-NR
Kiranyaz et al. [8] [2014]	Time, frequency and time frequency features were extracted	21-18	No cross-validation, 25% data for training	94.71-89.01-NR
Fürbass et al. [58] [2015]	EpiScan, an automatic method for seizure detection	23-NR	NR	NR-67-NR
Samiee et al. [10] [2015]	Multivariate textural features were extracted from gray level co-occurrence matrix	23-23	No cross-validation, 25% data for training	97.74-70.19-NR
Zabihi et al. [9] [2016]	7 features were extracted from intersection sequence of Poincaré section with phase space	23-23	25% training 50% training	93.21-88.27-93.11 94.80-89.10-94.69
This work	3 features extracted from different oscillatory levels using multivariate extension of EWT	23-5	Ten fold cross-validation	99.57-97.91-99.41

99.90% has been reported for patients 6 and 9 respectively using RF classifier. This implies that, the proposed method can distinguish the seizure-free epochs from seizure epochs effectively. For patient 6, the reason of high specificity may be due to the number of seizure-free instances are very high as compared to seizure instances, even after applying minority over sampling method. For most of the patients, the performance of the RF classifier has been found superior than other five studied classifiers, as the achieved average sensitivity, specificity and AUC values are the highest among all the classifiers. The FT classifier shows slight inferior performance than RF classifier. In the comparison between C4.5 and FT classifier, it is shown that, FT classifier performs slightly better than C4.5 classifier. Average sensitivity and specificity rate obtained for FT classifier are 95.58% and 99.30% respectively, whereas average sensitivity and specificity rate reported for C4.5 classifiers are 95.44% and 99.09% respectively. The performance of K-NN classifier in evaluating the proposed algorithm is also noteworthy as the obtained average sensitivity and specificity rates are 94.02% and 98.82% respectively. The sensitivity rate of K-NN classifier is less for patient 6 (only 77.6% seizures are truly classified) but it maintains high specificity rate (99.6%) for this patient. For patients 7, 11, 19 and 23, K-NN classifier achieved very good sensitivity rates (more than 99%) with high specificity rates. The Bayes-net classifier also provided good sensitivity and specificity rates for most of the patients. The average sensitivity and specificity rates for Bayes-net classifier are 91.93% and 98.70% respectively. The performance of Bayes-net classifier falls significantly in evaluating the proposed method for patient 15, as it achieved the lowest sensitivity rate of 71.3% with a specificity rate of

92.9%. The linear probabilistic Naive-Bayes classifier works with high sensitivity rates for few patients but it fails to maintain high specificity rates for those patients. However, for patient 7, 9 and 19, the Naive-Bayes classifier provided good sensitivity and specificity rates. The obtained average sensitivity, specificity and AUC for Naive-Bayes classifier are 88.46%, 95.74% and 0.981 respectively which are significantly less as compared to other five studied classifiers. For patients 6, 14 and 15, the sensitivity rates fall to less than 70% using Naive-Bayes classifier. However, it is clear from Table III that the sensitivity of proposed method is comparatively less for the patients 6, 13, 14, 15, and 16 using most of the classifiers. For those patients, the seizure segments are very hard to identify in the hour long record, the reason may be as follows: noise level is very high in seizure-free segments, recordings are highly contaminated with artifacts, seizure durations are too short to identify, as an example patient 16 had minimum seizure duration of 7 seconds. The proposed method detected most of the seizure epochs for patient 11, where maximum seizure duration was of 753 seconds, which is generally unusual. Thus the method could be applicable for the detection of long duration seizure events. To present the effectiveness of the proposed feature processing method, we have plotted the ROC curve for patient 1 using different JFs and their combination, shown in Fig. 10. For patient 1, JF1 performed the best among three JFs. The JF3 performed better than JF2 and combining these three JFs, the AUC increased significantly. Though, it is difficult to compare the proposed method with the existing methods, as all the methods are unique in selecting number of EEG channels, the number of features extracted, the feature processing stage, classification frame-work, we have put most

of the seizure detection methods (applied on CHB-MIT scalp EEG database) in Table IV. In Table IV, NR stands for not reported values. It has been reported that, the proposed method achieved increased sensitivity and specificity, which are significantly higher than all the existing methods reported in Table IV. This may be due to two main reasons firstly the previous methods used separate training and testing data, which may cause over-fitting problem. If the training features are from noisy or artifact contaminated EEG signals, then the classifier will not perform well in the testing data. Secondly, the number of seizure epochs are too less as compared to seizure-free epochs as discussed in the previous section, which may be a serious cause of over-fitting and classifiers will be biased to detect majority class, resulting into a lesser sensitivity rate. The proposed method uses only five automatically selected channels for EEG seizure detection with good performance. In addition, the performance of the proposed feature extraction method has been evaluated using only a single layer classifier architecture, which overcomes the issue of parallel processing and cloud computing. **The proposed multivariate extension of EWT generates time-frequency plane for multivariate signals.** Thus, with proper segmentation of the time-frequency plane and comparing the computed energy in 30-50 Hz frequency band with threshold energy level, SWD may also be detected from EEG signals.

VIII. CONCLUSION

In this paper, a novel seizure detection algorithm has been proposed, which is able to analyse multivariate non-stationarity EEG signals. The EWT has been explored in a novel way for multivariate signals. The time-frequency representation for multivariate multi-component signals is presented using multichannel extension of EWT. The proposed seizure detection method makes use of five EEG channels selected automatically using a novel channel selection method. Three features have been extracted from different oscillatory levels of multivariate EEG signals followed by a proposed feature processing method. The proposed feature processing method is found very effective to distinguish seizure events in long EEG recordings of hours duration. The reduction of feature dimensionality, prior to classification could be considered as a crucial step for automated classification of seizure and seizure-free EEG signals. Finally, the performance of the method has been evaluated using six well known classifiers, which have shown comparable performance among the other seizure detection methods studied on CHB-MIT database. In future, the proposed method can also be tested in intracranial EEG database of long duration recordings.

REFERENCES

- [1] H. Witte et al, "Special issue on epileptic seizure prediction," *IEEE Transactions on Biomedical Engineering*, vol. 50, no. 5, pp. 537–539, May 2003.
- [2] I. Osorio et al, "Real-time automated detection and quantitative analysis of seizures and short-term prediction of clinical onset," *Epilepsia*, vol. 39, no. 6, pp. 615–627, 1998.
- [3] N. S. O'Neill et al, "Identification of the temporal components of seizure onset in the scalp EEG," *The Canadian Journal of Neurological Sciences*, vol. 28, no. 03, pp. 245–253, 2001.
- [4] A. J. Gabor et al, "Automated seizure detection using a self-organizing neural network," *Electroencephalography and Clinical Neurophysiology*, vol. 99, no. 3, pp. 257–266, 1996.
- [5] A. J. Gabor, "Seizure detection using a self-organizing neural network: validation and comparison with other detection strategies," *Electroencephalography and Clinical Neurophysiology*, vol. 107, no. 1, pp. 27 – 32, 1998.
- [6] C. W. Hesse and C. J. James, "Tracking and detection of epileptiform activity in multichannel ictal EEG using signal subspace correlation of seizure source scalp topographies," *Medical & Biological Engineering & Computing*, vol. 45, no. 10, pp. 909–916, 2007.
- [7] A. Shoeb and J. Guttag, "Application of machine learning to epileptic seizure detection," in *Proceedings of the 27th International Conference on Machine Learning*, 2010, pp. 975–982.
- [8] S. Kiranyaz et al, "Automated patient-specific classification of long-term electroencephalography," *Journal of Biomedical Informatics*, vol. 49, pp. 16–31, 2014.
- [9] M. Zabihi et al, "Analysis of high-dimensional phase space via Poincaré section for patient-specific seizure detection," *IEEE Transactions on Neural Systems and Rehabilitation Engineering*, vol. 24, no. 3, pp. 386–398, 2016.
- [10] K. Samiee et al, "Long-term epileptic EEG classification via 2D mapping and textural features," *Expert Systems with Applications*, vol. 42, no. 20, pp. 7175 – 7185, 2015.
- [11] E. Sitnikova et al, "Sleep spindles and spikewave discharges in EEG: Their generic features, similarities and distinctions disclosed with Fourier transform and continuous wavelet analysis," *Journal of Neuroscience Methods*, vol. 180, no. 2, pp. 304 – 316, 2009.
- [12] A. Ovchinnikov et al, "An algorithm for real-time detection of spike-wave discharges in rodents," *Journal of Neuroscience Methods*, vol. 194, no. 1, pp. 172 – 178, 2010.
- [13] E. Sitnikova et al, "Time-frequency characteristics and dynamics of sleep spindles in WAG/Rij rats with absence epilepsy," *Brain Research*, vol. 1543, pp. 290 – 299, 2014.
- [14] A.I. Nazimov et al, "Serial identification of EEG patterns using adaptive wavelet-based analysis," *The European Physical Journal Special Topics*, vol. 222, no. 10, pp. 2713–2722, 2013.
- [15] G. V. Luijtelaar et al, "Methods of automated absence seizure detection, interference by stimulation, and possibilities for prediction in genetic absence models," *Journal of Neuroscience Methods*, vol. 260, pp. 144 – 158, 2016.
- [16] J. M. Lilly and S. C. Olhede, "Analysis of modulated multivariate oscillations," *IEEE Transactions on Signal Processing*, vol. 60, no. 2, pp. 600–612, 2012.
- [17] A. Ahrabian et al, "Synchrosqueezing-based time-frequency analysis of multivariate data," *Signal Processing*, vol. 106, pp. 331 – 341, 2015.
- [18] A. Ahrabian and D. P. Mandic, "Selective time-frequency reassignment based on synchrosqueezing," *IEEE Signal Processing Letters*, vol. 22, no. 11, pp. 2039–2043, 2015.
- [19] J. Gilles, "Empirical wavelet transform," *IEEE Transactions on Signal Processing*, vol. 61, no. 16, pp. 3999–4010, 2013.
- [20] S. Maheshwari et al, "Automated diagnosis of glaucoma using empirical wavelet transform and correntropy features extracted from fundus images," *IEEE Journal of Biomedical and Health Informatics*, In press 2016.
- [21] A. Bhattacharyya et al, "A novel approach for automated detection of focal EEG signals using empirical wavelet transform," *Neural Computing and Applications*, In press 2016.
- [22] A. L. Goldberger et al, "Physiobank, physiotoolkit, and physionet components of a new research resource for complex physiologic signals," *Circulation*, vol. 101, no. 23, pp. e215–e220, 2000.
- [23] A. H. Shoeb, "Application of machine learning to epileptic seizure onset detection and treatment," Ph.D. dissertation, Massachusetts Institute of Technology, 2009.
- [24] N. F. Chang et al, "Channel selection for epilepsy seizure prediction method based on machine learning," in *Annual International Conference of the IEEE Engineering in Medicine and Biology Society*, 2012, pp. 5162–5165.
- [25] S. Li et al, "Seizure prediction using spike rate of intracranial EEG," *IEEE Transactions on Neural Systems and Rehabilitation Engineering*, vol. 21, no. 6, pp. 880–886, 2013.
- [26] B. Atoufi et al, "A survey of multi-channel prediction of EEG signal in different EEG state: normal, pre-seizure, and seizure," in *Proceedings of the Seventh International Conference on Computer Science and Information Technologies*, Yerevan, Armenia, 2009.

- [27] M. S. Roulston, "Estimating the errors on measured entropy and mutual information," *Physica D: Nonlinear Phenomena*, vol. 125, no. 3, pp. 285–294, 1999.
- [28] Daubechies, Ingrid et al, *Ten Lectures on Wavelets*, 1992, vol. 61.
- [29] A. E. Hramov et al, *Wavelets in Neuroscience*. Springer, 2015.
- [30] N. E. Huang et al, "The empirical mode decomposition and the Hilbert spectrum for nonlinear and non-stationary time series analysis," in *Proceedings of the Royal Society of London A: Mathematical, Physical and Engineering Sciences*, vol. 454, no. 1971, 1998, pp. 903–995.
- [31] N. E. Huang, *Hilbert-Huang transform and its applications*. World Scientific, 2014, vol. 16.
- [32] E. Bacry et al, "Wavelet analysis of fully developed turbulence data and measurement of scaling exponents," in *Turbulence and Coherent Structures*. Springer, 1991, pp. 203–215.
- [33] N. E. Huang and Z. Wu, "A review on Hilbert-Huang transform: Method and its applications to geophysical studies," *Reviews of Geophysics*, vol. 46, no. 2, 2008.
- [34] T. Inouye et al, "A new segmentation method of electroencephalograms by use of Akaike's information criterion," *Cognitive Brain Research*, vol. 3, no. 1, pp. 33–40, 1995.
- [35] J. A. McEwen and G. B. Anderson, "Modeling the stationarity and gaussianity of spontaneous electroencephalographic activity," *IEEE transactions on Biomedical Engineering*, no. 5, pp. 361–369, 1975.
- [36] A. A. Fingelkurs et al, "Interictal EEG as a physiological adaptation. Part I. Composition of brain oscillations in interictal EEG," *Clinical neurophysiology*, vol. 117, no. 1, pp. 208–222, 2006.
- [37] D. Kugiumtzis and A. Tsimpiris, "Measures of Analysis of Time Series (MATS): A MATLAB Toolkit for Computation of Multiple Measures on Time Series Data Bases," *Journal of Statistical Software*, vol. 33, no. i05, 2010.
- [38] H. Kawahara et al, "Restructuring speech representations using a pitch-adaptive timefrequency smoothing and an instantaneous-frequency-based F0 extraction: Possible role of a repetitive structure in sounds," *Speech Communication*, vol. 27, no. 34, pp. 187 – 207, 1999.
- [39] P. Ren et al, "Gait rhythm fluctuation analysis for neurodegenerative diseases by empirical mode decomposition," *IEEE Transactions on Biomedical Engineering*, vol. PP, no. 99, pp. 1–1, 2016.
- [40] N. V. Chawla et al, "SMOTE: synthetic minority over-sampling technique," *Journal of Artificial Intelligence Research*, pp. 321–357, 2002.
- [41] L. Victoria et al, "Analysis of preprocessing vs. cost-sensitive learning for imbalanced classification. Open problems on intrinsic data characteristics," *Expert Systems with Applications*, vol. 39, no. 7, pp. 6585 – 6608, 2012.
- [42] L. Breiman, "Random forests," *Machine learning*, vol. 45, no. 1, pp. 5–32, 2001.
- [43] J. R. Quinlan, *C4. 5: programs for machine learning*. Elsevier, 2014.
- [44] J. Gama, "Functional trees," *Machine Learning*, vol. 55, no. 3, pp. 219–250, 2004.
- [45] J. Luo et al, "A Bayesian network-based framework for semantic image understanding," *Pattern Recognition*, vol. 38, no. 6, pp. 919–934, 2005.
- [46] A. Jordan, "On discriminative vs. generative classifiers: A comparison of logistic regression and Naive-Bayes," *Advances in neural information processing systems*, vol. 14, p. 841, 2002.
- [47] D. W. Aha et al, "Instance-based learning algorithms," *Machine Learning*, vol. 6, no. 1, pp. 37–66, 1991.
- [48] M. Hall et al, "The WEKA data mining software: an update," *ACM SIGKDD Explorations Newsletter*, vol. 11, no. 1, pp. 10–18, 2009.
- [49] R. Kohavi et al, "A study of cross-validation and bootstrap for accuracy estimation and model selection," in *Ijcai*, vol. 14, no. 2, 1995, pp. 1137–1145.
- [50] E. C. P. Chua et al, "Improved patient specific seizure detection during pre-surgical evaluation," *Clinical Neurophysiology*, vol. 122, no. 4, pp. 672 – 679, 2011.
- [51] B. R. Greene et al, "Electrocardiogram based neonatal seizure detection," *IEEE Transactions on Biomedical Engineering*, vol. 54, no. 4, pp. 673–682, 2007.
- [52] A. T. Azar and S. A. El-Said, "Performance analysis of support vector machines classifiers in breast cancer mammography recognition," *Neural Computing and Applications*, vol. 24, no. 5, pp. 1163–1177, 2014.
- [53] R. Sharma, and R. B. Pachori, "Classification of epileptic seizures in EEG signals based on phase space representation of intrinsic mode functions," *Expert Systems with Applications*, vol. 42, no. 3, pp. 1106 – 1117, 2015.
- [54] N. Rafiuddin et al, "Feature extraction and classification of eeg for automatic seizure detection," in *International Conference on Multimedia, Signal Processing and Communication Technologies*, 2011, pp. 184–187.
- [55] Y. U. Khan et al, "Automated seizure detection in scalp EEG using multiple wavelet scales," in *IEEE International Conference on Signal Processing, Computing and Control*, March 2012, pp. 1–5.
- [56] B Hunyadi et al, "Incorporating structural information from the multichannel EEG improves patient-specific seizure detection," *Clinical Neurophysiology*, vol. 123, no. 12, pp. 2352 – 2361, 2012.
- [57] A. Supratak et al, "Feature extraction with stacked autoencoders for epileptic seizure detection," in *36th Annual International Conference of the IEEE Engineering in Medicine and Biology Society*, 2014, pp. 4184–4187.
- [58] F. Fürbass et al, "Prospective multi-center study of an automatic online seizure detection system for epilepsy monitoring units," *Clinical Neurophysiology*, vol. 126, no. 6, pp. 1124 – 1131, 2015.